

CEOCOR DRESDEN – SECTOR A

Paper n. 10

AC INTERFERENCE ON A GAS PIPELINE CAUSED BY NEARBY POWER LINES IN A COMPLEX RIGHT-OF-WAY

COMPARISON BETWEEN MEASUREMENTS AND CALCULATIONS

G. C. Christoforidis, D. P. Labridis, P. S. Dokopoulos
Aristotle University of Thessaloniki,
Power Systems Laboratory,
P.O. Box 486
541 24 Thessaloniki, Greece,
email: gchristo@auth.gr

N. Kioupis
Public Gas Corporation of Greece (DEPA) S.A.,
207 Messoyion Ave.,
115 25 Athens, Greece,
email: n.kioupis@depa.gr

Abstract

The interference caused by power transmission lines to buried gas pipelines is under investigation for many years. Situations where a pipeline is influenced by more than one power lines are more frequent nowadays, thus making the interaction more complex. Even under normal operating conditions, voltages and currents are induced on the pipeline that may pose danger to working personnel or may accelerate the corrosion of the pipeline's metal. In this paper, a case study taken from the Greek Transmission System is demonstrated. Measurements of the induced voltage at certain locations of a pipeline section are compared with theoretical calculations. These calculations comprise finite element computations and circuit analysis. Results presented show that the induced voltage on the pipeline is heavily influenced on the loading of each of the power lines, which must be known throughout the common route. For an accurate calculation of the induced parameters, it is recommended that the coupling between all conductors of the problem should be taken into consideration. Furthermore, theoretical calculations presented show the influence of the operation of installed over-voltage arresters, which connect the pipeline to mitigation grounding wires.

Key Words

Finite element methods, gas pipelines, inductive interference, power transmission lines.

1. Introduction

The situations where a buried gas pipeline and one or more power transmission lines share proximal rights-of-way for considerable lengths are very common nowadays. The main reasons for that are the high cost of rights-of-way suitable for pipelines and power lines, the environmental restrictions imposed to public utilities and the ever-increasing energy consumption. In such cases, the buried pipeline is subject to an electromagnetic interference caused by the neighbouring power line(s). This interference generally consists of an inductive, a conductive and a capacitive part. The capacitive component is ignored for buried pipelines, whereas the conductive part is present only under fault conditions and affects the part of the pipeline that is close to the faulted structure. The inductive component, which is the result of the magnetic field generated by a power line, is present both during faults and normal operating conditions and is the dominant one.

Due to the inductive interference, voltages and currents are induced in a buried metallic pipeline. The high quality of present pipeline coatings results in higher induced voltages. These voltages should be kept below certain levels imposed by various standards and regulations. The most recent NACE standard [1] suggests that under normal operating conditions the induced voltage on a pipeline should not exceed 15 V, in order to minimize the possibility of AC corrosion and to ensure personnel safety.

The problem of electromagnetic interference between power lines and buried pipelines has attracted many researchers during the past 40 years. Initially, the attempts to develop a suitable calculation method for this interference were based on the Carson's relations [2] or similar improved ones [3-6]. A technical recommendation was issued in Germany based on these works, which was revised later [7] including useful charts that may be utilized for simple problems. With the advances in computer technology, more sophisticated models were adopted, leading to more accurate methods of calculation [8-10], that may be used to solve complex problems. A general guide on the subject was issued later by CIGRE [11], while CEOCOR published a report focusing on the AC corrosion of pipelines due to the influence of power lines [12]. More recently, a hybrid method utilizing the Finite-Element Method (FEM) and circuit theory was introduced [13, 14]. This method removed certain simplifications of previous methods, being able to accurately solve the problem regardless of

geometrical complexity, the number of conductors or the presence of mediums with different electromagnetic properties.

In this work, the application of this method to a real situation encountered in the Greek network is presented. The results of the theoretical calculations are compared to measurements in order to validate the approach. The paper gives valuable information about the interaction between three power transmission lines and a buried pipeline sharing a complex right-of-way. Previous published works and reports have not dealt with such a complex situation and its particular characteristics.

2. Description of Right-Of-Way

A map of the routes of the pipeline section under investigation and the power lines that influence it is shown in Fig.1. This right-of-way is located at the general Theba area in Greece. The northern end of the pipeline section is located near Aliartos town of Viotia, whereas the southern end is near Dafni village. As it may be realised, the simplification of a parallel exposure cannot be adopted here. There exist several crossings between the pipeline and the power lines and, moreover, in many sections the pipeline is not parallel to the power lines. In these cases, a conversion of the non-parallel exposure or crossing to an equivalent parallel exposure should be made, according to the ITU directives [15].

The above pipeline section is part of a natural gas transmission main, installed between 1993 and 1995. The burial depth of the pipeline is between 1 m and 2 m, its outside diameter is 762 mm and its wall thickness ranges from 9.52 mm and 15.6 mm. The pipeline is coated with fused bonded epoxy primer and three-layer extruded polyethylene. The coating resistance is considered to be $1000 \text{ k}\Omega\cdot\text{m}^2$. The overall length of this pipeline section is 36 km approximately, and is electrically separated from the rest line by buried insulating joints at both ends. Mitigation grounding wires are installed at strategic locations in this section, in parallel to the pipeline. The pipeline is connected to the grounding wires via six semiconducting over-voltage arresters that operate when the AC voltage between the pipeline and earth exceeds the value of 25 V. The mitigation performance of these arresters was demonstrated in [16] by real-time measurements. The pipeline is equipped with 36 cathodic protection test posts named “KG” allowing measurements of potential and line current. The over-voltage arresters are installed at both ends of the pipeline section and at test points KG 82.263 km, KG 71.463 km, KG 56.563 km and KG 51.763 km.

The power lines that influence this section of the gas pipeline are:

- A 400 kV double circuit line, named “Athens-Acheloos” (AA), having two or three ground wires,
- An 150 kV double circuit line, named “Aluminio-Rouf” (AR), having one or two ground wires,
- An 150 kV single circuit line, named “Schimatari-Larisa” (SL), having two or three ground wires.

The geometrical configurations of these three power lines are shown in Fig.2. The additional ground wire at each of the towers is located at the base of the tower. It should be noted that the loading of the power lines might not constant throughout the common route, as heavy loads, like the city of Theba, are located approximately at the midst of the route.

An equivalent earth resistivity equal to $54 \Omega\cdot\text{m}$ is considered throughout the route, based on previous measurements.

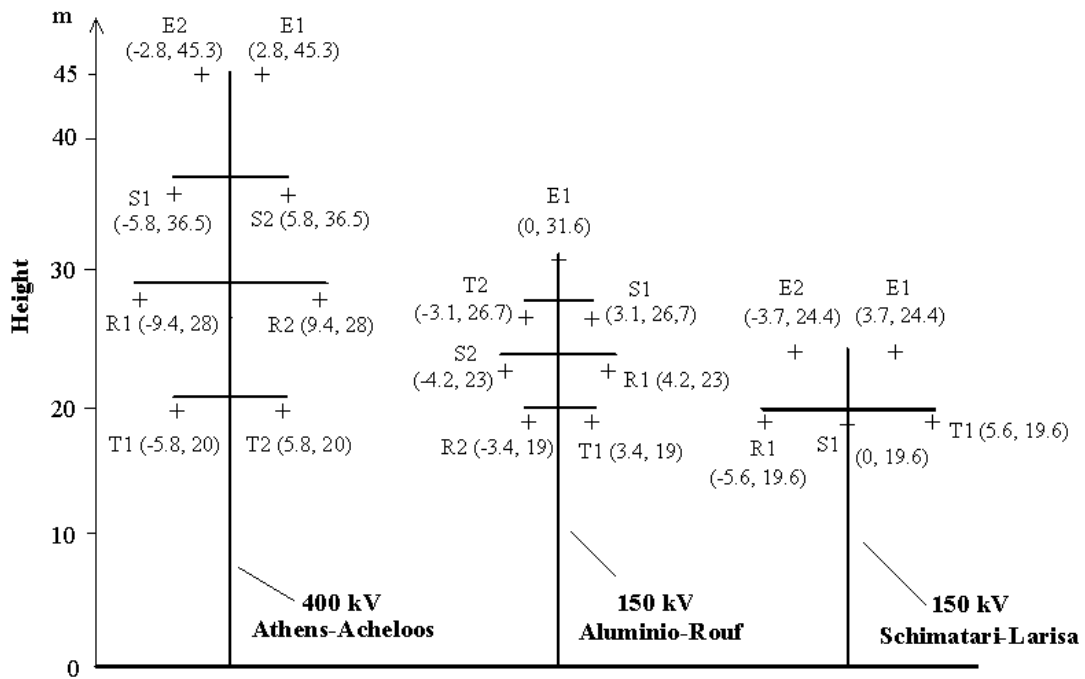


Figure 2: Transmission lines configurations

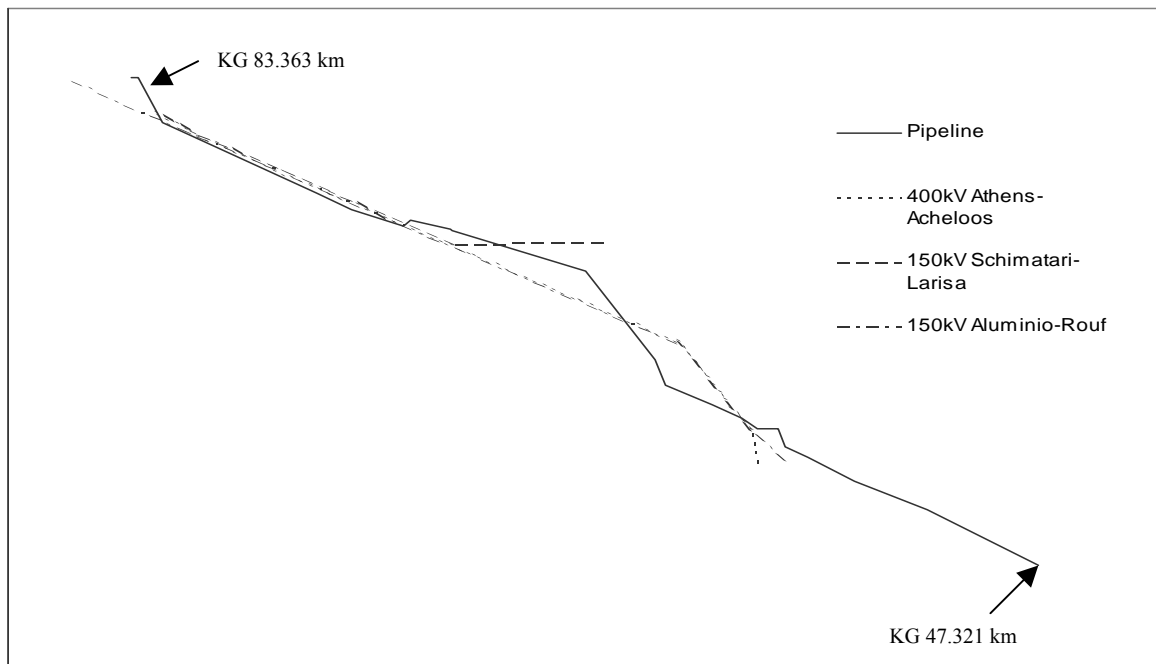


Figure 1: Map of right-of-way shared by the pipeline and three power transmission lines.

3. Experimental Procedure

The field measurements were conducted between 21/1/2004 and 28/1/2004 at selected locations on the pipeline section. The recording of the AC voltage was performed using “Weilekes Elektronik Minilog 512Kbyte” on the 30V AC range (input resistance: 1M Ω). This recorder was a two-channel data logger, with a built-in AC-filter, which allowed simultaneous recording of DC and AC voltage. The sampling rate was set at 10 sec. Five data loggers of this type were installed at certain test posts of the pipeline. These test posts were

located at both ends of the pipeline section and at locations KG 59.3 km, KG 71.845 km and KG 73.6 km respectively.

The measurements of the transmission line currents were taken from HTSO historical recorded data. Line currents are measured at switches of certain substations and are collected in a database as recorded data in one-minute intervals. Only the current of one phase of each line is measured and, therefore, there is no knowledge of possible unbalanced loading. The closest measurement stations were at substation Schimatari for the 150 kV Schimatari-Larisa line and at substations Koumoundourou and Distomo for the other two lines.

4. Description of Calculation Method

The calculation method for the induced voltages on a pipeline is a hybrid one and comprises four steps. For a detailed description the reader may refer to [13]. The required input data for the method are the geometrical configurations of power lines and pipeline, the physical characteristics of the conductors, the earth and the pipeline and loading of the power lines.

A. Determination of the Equivalent Exposure

The calculation method can be applied directly only to parallel exposures. If the interpretation of a parallel exposure is not applicable, as in the case study of this paper, a conversion to an equivalent parallel exposure is made, according to the ITU directives [15].

There are generally two categories of non-parallel exposures:

- Oblique exposures and
- Crossings

An oblique exposure, as the one shown in Fig.3, may be considered as a parallel section having a relative distance a from the power line equal to:

$$a = \sqrt{a_1 a_2} \quad (1a)$$

$$\text{as long as } \frac{a_2}{a_1} \leq 3 \quad (1b)$$

In case $\frac{a_2}{a_1}$ is more than 3, the section is divided, as shown in Fig.3, in order that both $\frac{a_3}{a_1}$ and

$\frac{a_2}{a_3}$ meet (1b).

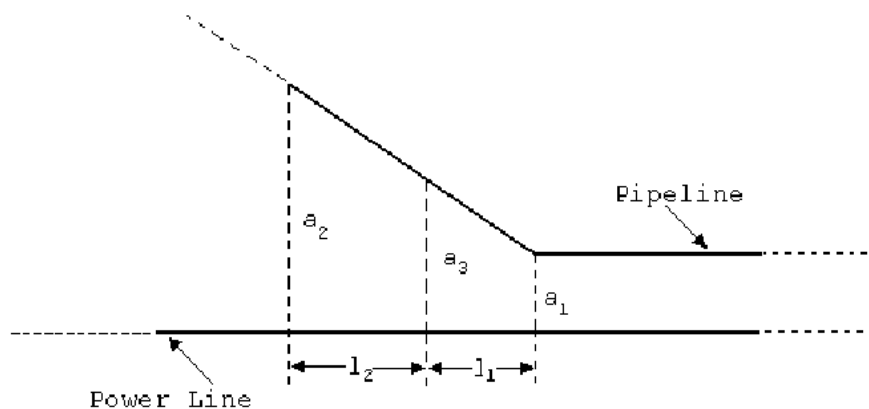


Figure 3: Example of an oblique exposure

A crossing section may be treated as an equivalent parallel section having a separation distance of $d = 6$ m and a length which is equal to the projection of that segment of the pipeline that is within a zone of 10 m on both sides of the power line. This is illustrated in Fig.4.

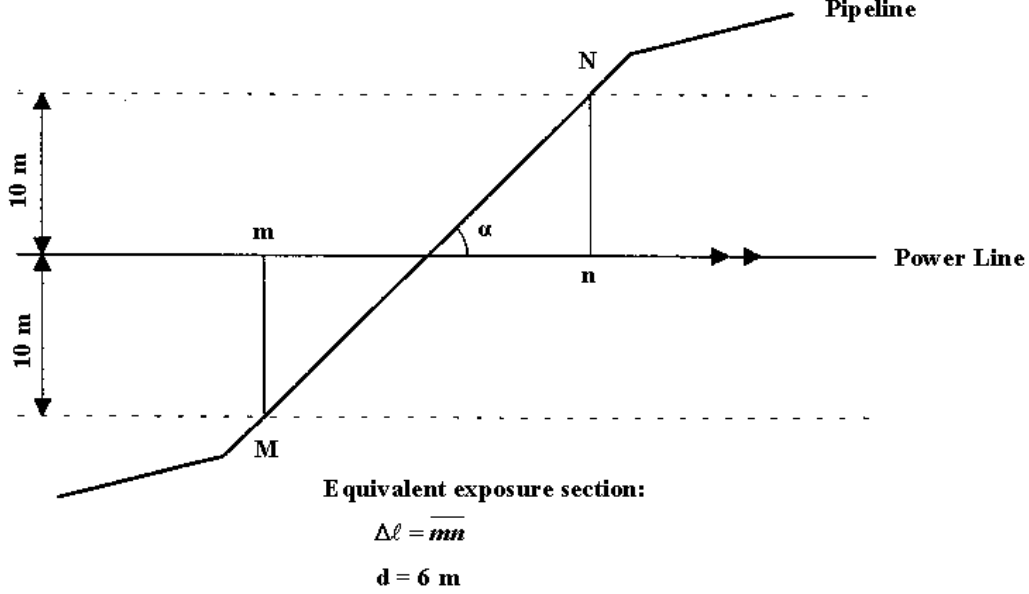


Figure 4: Conversion of a crossing section to an equivalent parallel one

Following this procedure a complex right-of-way is transformed into a series of equivalent sections with different relative distances between the pipeline and the power line(s). In these sections the pipeline may be considered parallel to the power lines(s).

B. Field Equations and Finite Element Formulation

A system of N infinitely long conductors, carrying rms currents I_i ($i=1, 2, \dots, N$) over imperfect earth is considered. Considering that the cross-section of the system under investigation lies on the x - y plane, the following system of equations describes the linear two-dimensional electromagnetic diffusion problem for the z -direction components \bar{A}_z of the Magnetic Vector Potential (MVP) and \bar{J}_z of the total current density vector [16]:

$$\frac{1}{\mu_0 \mu_r} \left[\frac{\partial^2 \bar{A}_z}{\partial x^2} + \frac{\partial^2 \bar{A}_z}{\partial y^2} \right] - j\omega\sigma \bar{A}_z + \bar{J}_{sz} = 0 \quad (1a)$$

$$-j\omega\sigma \bar{A}_z + \bar{J}_{sz} = \bar{J}_z \quad (1b)$$

$$\iint_{S_i} \bar{J}_z dS = \bar{I}_i \quad i = 1, 2, \dots, N \quad (1c)$$

where σ is the conductivity, μ_0 and μ_r are the vacuum and relative permeabilities respectively, ω is the angular frequency, \bar{J}_{sz} is the source current density in the z -direction and \bar{I}_i is the rms value of the current flowing through conductor i of cross-section S_i .

It is shown in [17] that the finite-element formulation of equations (1a-c) leads to a matrix equation. Using the solution of this matrix equation, the MVP values in every node of the discretization domain, as well as the unknown source current densities, are calculated. Therefore, for a random element e , the eddy-current density \bar{J}_{ez}^e is calculated using the relation:

$$\bar{J}_{ez}^e(x, y) = -j\omega\sigma\bar{A}_z^e(x, y) \quad (2a)$$

and the total element current density \bar{J}_z^e , being the sum of the conductor - i source current density \bar{J}_{szi} and of the element eddy current density \bar{J}_{ez}^e of (2a), is obtained by the following equation:

$$\bar{J}_z^e(x, y) = \bar{J}_{szi}^e(x, y) + \bar{J}_{szi} \quad (2b)$$

Integrating (2b) over a conductor cross-section, the total current flowing through this conductor is obtained.

A local error estimator, based on the discontinuity of the instantaneous tangential components of the magnetic field, has been chosen as in [18] for an iteratively adaptive mesh generation.

C. Determination of Self and Mutual Impedances of Conductors

Generally, if there exist n conductors in the configuration, the mutual complex impedance \bar{Z}_{ij} between conductor i and another conductor j carrying a certain current \bar{I}_j , where all other conductors are forced to carry zero currents, is given by:

$$\bar{Z}_{ij} = \frac{\bar{V}_i}{\bar{I}_j} \quad (i, j = 1, 2, \dots, N) \quad (3)$$

assuming that the per-unit length voltage drop \bar{V}_i on every conductor is known for a specific current excitation. Similarly, the self-impedance of conductor i may be calculated using (3), by setting $i = j$.

The procedure is summarized below [19]:

- By applying a sinusoidal current excitation of arbitrary magnitude to each conductor, while applying zero current to the other conductors, the corresponding voltages are calculated.
- The self and mutual impedances of the j conductor may be calculated using (3).

The above procedure is repeated n times, so as to calculate the impedances of n conductors.

The source current density \bar{J}_{szi} for every conductor i have been calculated by solving the system of equations 1a-1c. Therefore, equation (3) becomes [19]:

$$\bar{Z}_{ij} = \frac{\bar{V}_i}{\bar{I}_j} = \frac{\bar{J}_{szi} / \sigma_i}{\bar{I}_j} \quad (i, j = 1, 2, \dots, N) \quad (4)$$

Following the above procedure, effectively linking electromagnetic field variables and equivalent circuit parameters, the self and mutual impedances per unit length of the problem are computed.

D. Circuit Representation of the Problem

Having computed the impedances of the problem, a generalized equivalent circuit is constructed, as shown in [13]. In case the power line has two circuits, like the AA and AR lines of this case study, the equivalent circuit is that of Fig.5. Although it is not shown in this figure, the coupling between all conductors is taken into consideration. Also, it has to be noted that the connections to earth of the phase wires, due to their per-unit length capacitances to ground, are not neglected. In the circuit representation, the ground wires are replaced with an equivalent metallic return path. In order to account for the fact that the pipeline coating is not perfect, (i.e. it has defects), the pipeline is modeled in sections utilizing a series of

grounding-leakage resistances. These resistances may, also, represent regular groundings used as a mitigation measure, mainly ground or polarization cells.

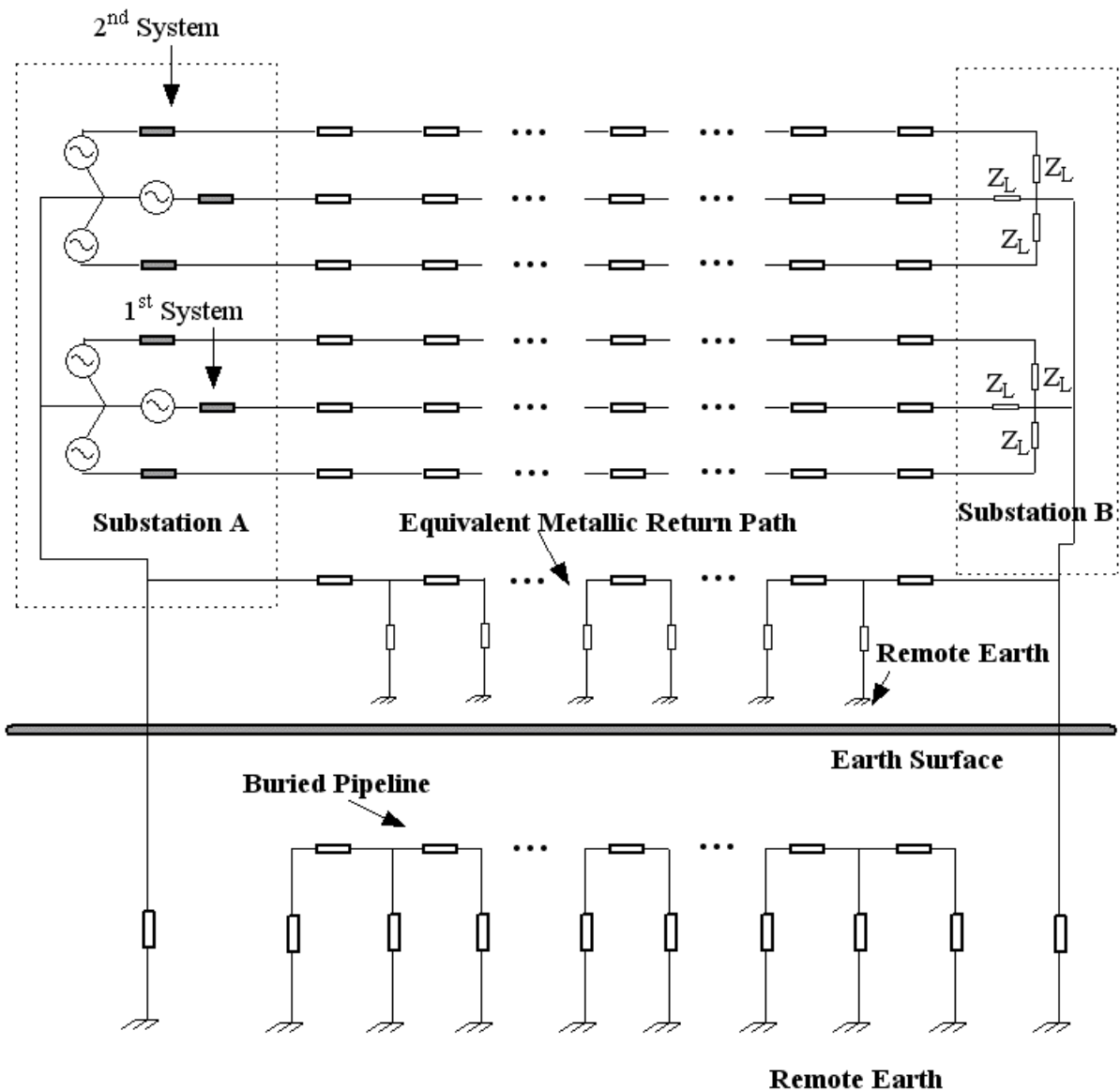


Figure 5: Circuit representation of the problem

In case more pipelines or lines exist in the configuration, they are modeled separately using the same procedure. Such cases exist in this case study, in the sections where all three power lines influence the pipeline. A system of equations is constructed and solved using standard methods available in literature, e.g. [20], giving the unknown currents in every section of the problem.

5. Results and Discussion

The common route showed in Fig.1 was split in 68 subsections of different lengths, in order to comply with the theory presented in subsection 4.A and the possible changes in the configuration of the power lines. There are subsections influenced by all power lines, others by one or two of the power lines and, towards the southern end, the pipeline is not under any influence from inducing sources. Therefore, this is a complex situation that depends on several parameters. For what concerns that amount of induced voltage on the pipeline, apart

from its intrinsic characteristics, the most important parameter is the loading of the power lines.

A. Comparison between measurements and calculations

Throughout the measurements the loading of the power lines varied considerably, which allowed for useful observations. The measured induced voltage did not exceed at any case the value of 25 V and, therefore, the over-voltage arresters remained inactive.

The highest value of 20.65 V was measured at the northern end of the pipeline on 23/1/2004 at 19:39 hours. At that time the loading of the two systems of the 400 kV line (AA) was 550 A and 500 A respectively, while both systems of the 150 kV AR line were loaded with 235 A approximately. The measured loading of the 150 kV SL line was 35 A at the Schimatari measuring point (i.e. closest to the southern end of the pipeline) and 287 A at the Lamia measuring point (i.e. closest to the northern end). In Fig.6 the comparison between the measured and the calculation values is shown. For the calculations, the loading of the SL line was assumed to be 35 A, which is the main reason of the relatively high difference between measurement and calculation at the northern end. The black bullets at the graphs depict the measured values of the induced voltage, while the continuous line represents the calculated induced voltage.

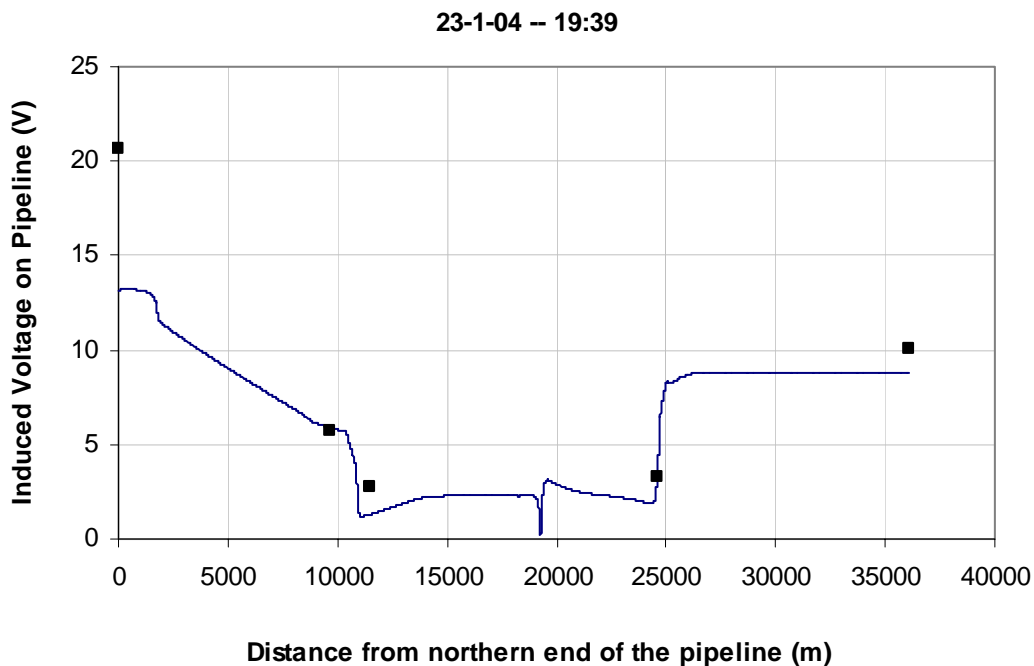


Figure 6: Comparison between measurements and calculations on 23-1-04 at 19:39 hours.

It was generally observed that the highest induced voltages on the pipeline were measured when the loading of the 400 kV AA line was near or at the maximum value. This may be realized by observing Fig.7 that shows the comparison between measurements and calculations on 22-1-2004 at 08:33 hours. The loading of the two systems of the AA line was 330 A and 305 A respectively, while the loading of the two systems of the AR line was 195 A and 187 A respectively. The measured loading of the SL line was 90 A at the Schimatari point and 130 A at the Lamia point. In this case the induced voltage is considerably lower than the previous one of Fig.6. Moreover, the difference between measurements and calculations at the northern end of the pipeline is lower also, stemming from the fact that the loading of the SL line varied less than before at the measuring points.

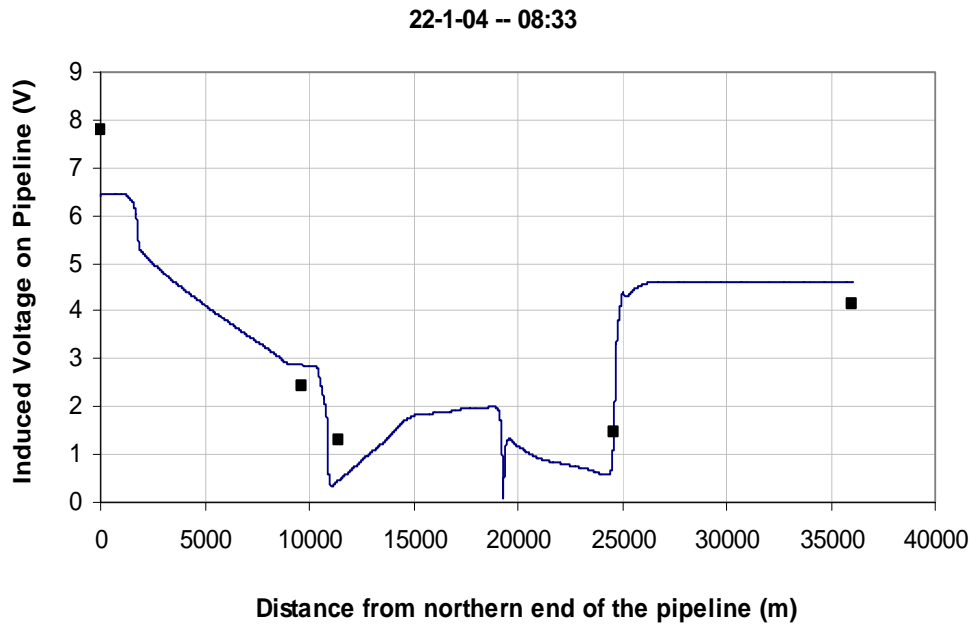


Figure 7: Comparison between measurements and calculations on 22-1-04 at 08:33 hours.

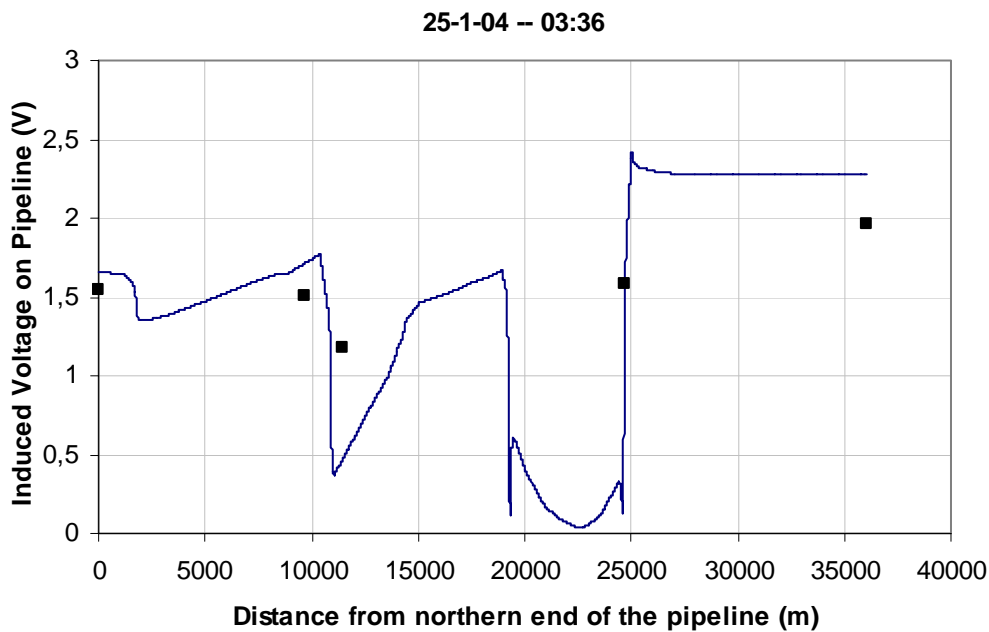


Figure 8: Comparison between measurements and calculations on 25-1-04 at 03:36 hours.

At most times the amount of induced voltage at the northern end of the pipeline was higher than that at the southern end. However, at certain times this was not true. An example of a such a situation were the measured voltage at the southern end was higher, is shown in Fig.8.

In this case, the shape of the induced voltage graph on the pipeline section differs from the previous ones. The main reason for these two variations is the low loading of the AR line, which is the line that influences the pipeline along most of the route. Specifically, at this time the loading of the two systems of the AR line was 50 A, while the loading of the two systems of the AA line was 265 A and 230 A respectively. The loading of the SL line was 85 A at the southern measuring point and 110 A at the northern point.

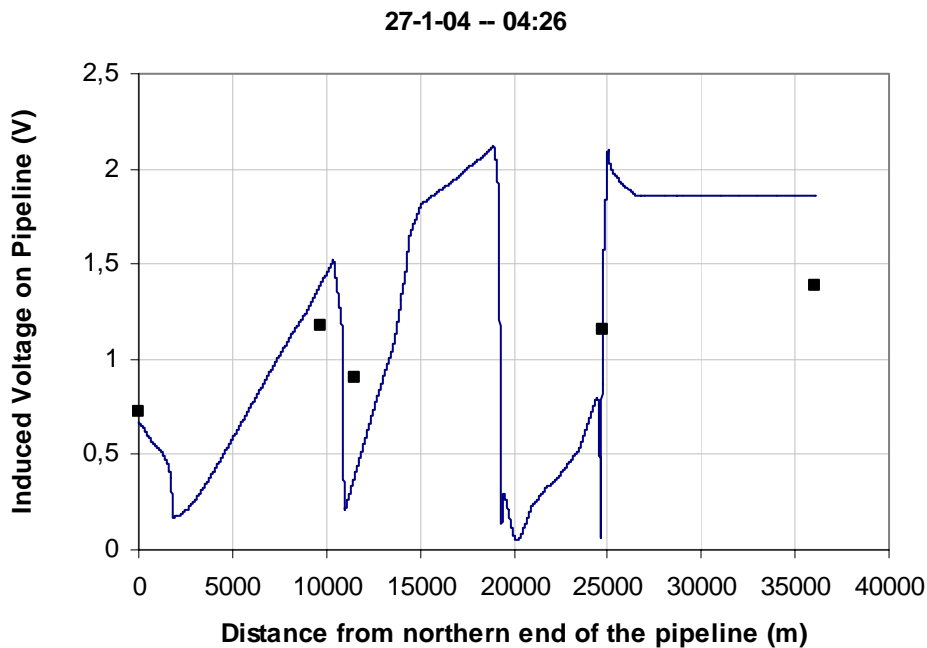


Figure 9: Comparison between measurements and calculations on 27-1-04 at 04:26 hours

The lowest measured voltage at the northern end was 0.72 V on 27-1-2004 at 04:26 hours. The corresponding comparison is shown in Fig.9. In this case, the loading of the SL line was almost uniform as the measurements at both ends of the line were 122 A, approximately. The loading of the two systems of the AA line was 282 A and 250 A respectively, while for the AR line was 60 A for both systems. In this case, the uniform loading of the SL line helps in a better convergence between measurements and calculations, whereas the low loading of the AR line reverses the peak of the induced voltage from the northern end to southern end.

B. Theoretical investigation of the behaviour of the over-voltage arresters

The influence of the over-voltage arresters could not be tested throughout the measurements, as the measured voltage never exceeded the value of 25 V at any point. Therefore, in this section some theoretical calculations are presented that show how the induced voltage profile on the pipeline section is influence by the triggering of the arresters. For the calculations, when the induced voltage exceeds the amount of 25 V at the locations of the arresters, it is assumed that a grounding with 2.5 Ω resistance is connected to the pipeline. For the test cases presented in the following figs.10 and 11, five arresters out of six operate.

Assuming that both the AR and AA lines are loaded with their maximum possible continuous loading, which is 778 A and 1920 A respectively, while the SL line is loaded with 21 A. All lines are assumed to have balanced loading. Fig.10 shows the reduction of the pipeline voltage when the over-voltage arresters operate. It may be observed that the induced voltage at the northern end is reduced 80% approximately, whereas the voltage does not exceed the safety limit of 15 V anywhere at the pipeline section.

Generally, the inclusion of the additional grounding resistances in the equivalent circuit, corresponding to the connection of the pipeline to the grounding mitigation wire via the over-voltage arresters, results in considerable variation in the induced voltage profile on the pipeline. This may be realised by inspecting both fig.10 and fig.11, where all pipelines are

loaded with their maximum possible continuous loading. The maximum loading of the SL line is 600 A. Particularly in fig.11, the induced voltage profile changes in a way that the voltage exceeds the safety limit of 15 V at a certain part of the pipeline, although this is not true when the arresters do not operate. Consequently, a detailed and careful investigation of all possible situations, regarding mitigation measures, is necessary, in order to avoid similar situations.

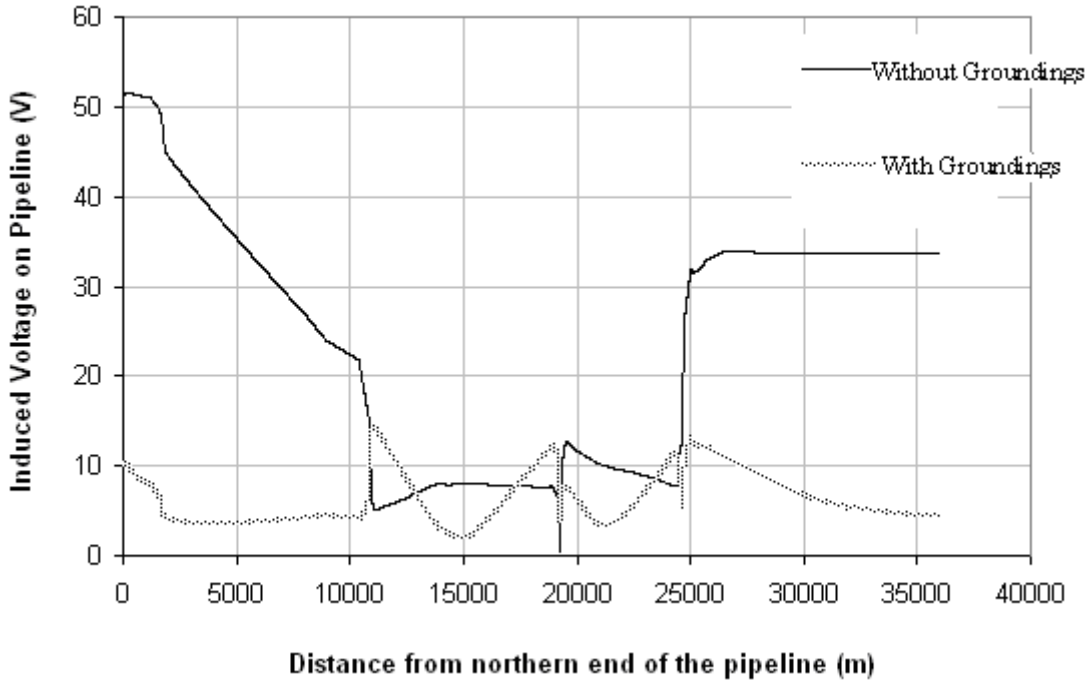


Figure 10: Calculated profile of the induced voltage on the pipeline section for maximum loading of the AR and AA lines and a loading of 21 A of the SL line, with or without the over-voltage arresters.

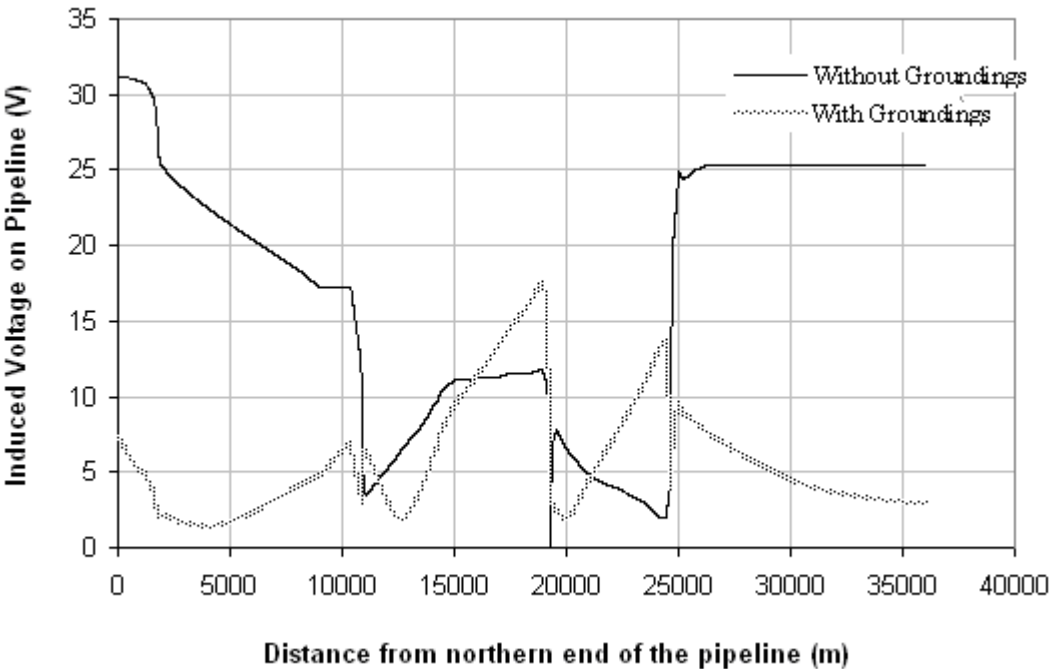


Figure 11: Calculated profile of the induced voltage on the pipeline section for maximum loading of all the power lines, with or without the over-voltage arresters.

However, practical experience have shown that when over voltage occurs on the pipeline, only one or both the arresters located at both ends of the section may operate. This may be explained by the fact that the graphs in figs 10 and 11 correspond to the worst normal operating conditions. In case only the terminal arresters, located at both ends of the pipeline section operate, due to failure of triggering of the other three, the induced voltage is still reduced significantly. This may be realized by the following graphs, shown in figs.12 and 13, which show the result of the operation of only the terminal arresters, for the two theoretical cases discussed above.

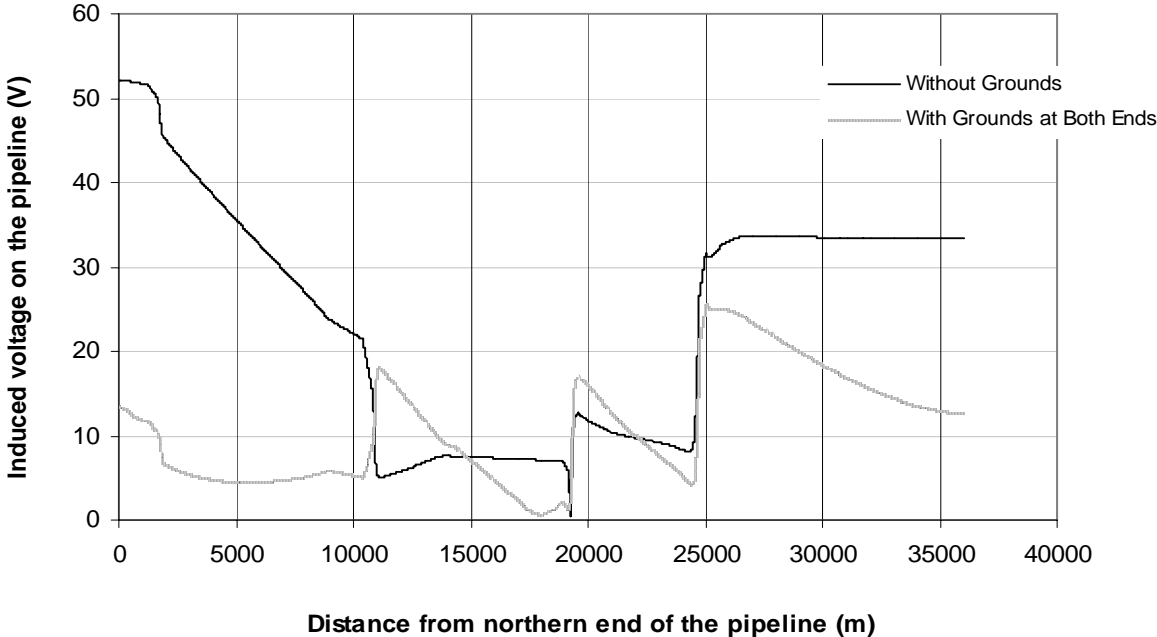


Figure 12: Calculated profile of the induced voltage on the pipeline section for maximum loading of the AR and AA lines and a loading of 21 A of the SL line, without the over-voltage arresters or with only the terminal arresters operating.

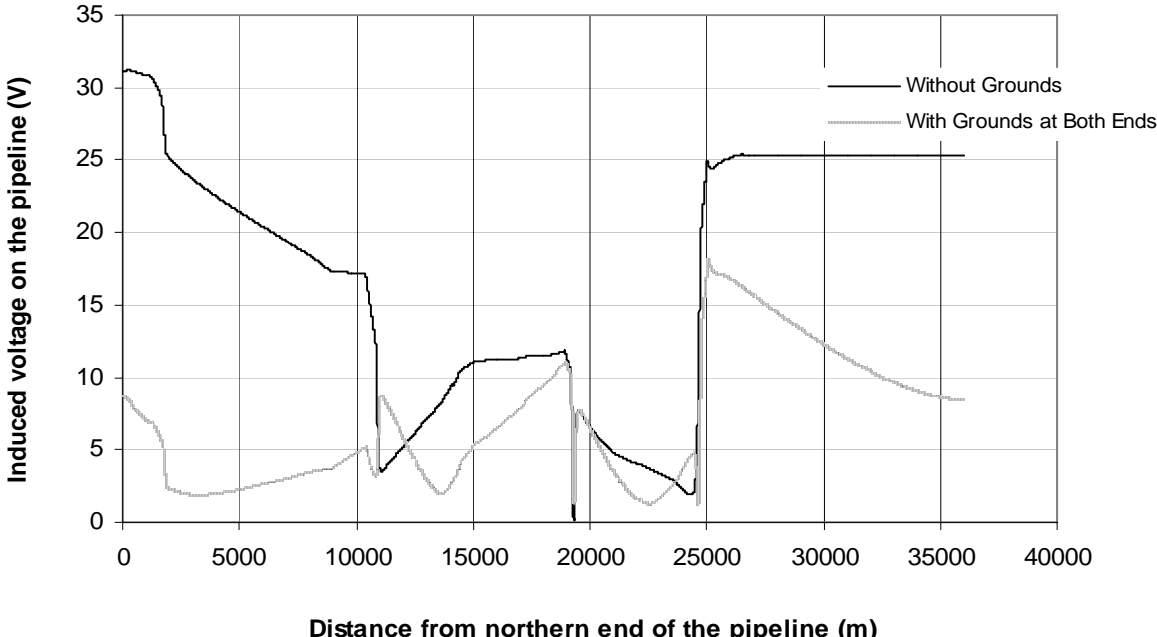


Figure 13: Calculated profile of the induced voltage on the pipeline section for maximum loading of all the power lines, without the over-voltage arresters or with only the terminal arresters operating.

6. Conclusions

A case study regarding the influence of three power lines to a buried pipeline, taken from the Greek network, has been examined in this paper. Measurements of the pipeline voltage, which were conducted recently at certain locations of a pipeline section, have been compared with theoretical calculations using a hybrid method comprising FEM calculations and circuit analysis. The importance of accurately modeling the common route of the power lines and pipeline has been highlighted. The complexity stemming from the simultaneous coupling between all power lines and the pipeline, results in a voltage profile that is very sensitive to the loading of each power line. Therefore, in order to calculate accurately the voltage profile, the knowledge of the loading of the power lines throughout the right-of-way is necessary. Moreover, the influence of the operation of the over-voltage arresters that connect the pipeline with mitigation grounding wires is demonstrated at certain theoretical situations. It is concluded that a detailed investigation of the possible situations, concerning the loading of the interfering power lines, should be performed.

References:

- [1] Mitigation of alternating current and lightning effects on metallic structures and corrosion control systems, NACE Standard RP0177-95.
- [2] J. R. Carson, Wave propagation in overhead wires with ground return., *Bell System Technical Journal*, Vol. 5: 539-554, 1926.
- [3] H. Böcker, D. Oeding, Induktionsspannung an Pipelines in trassen von hochspannungsleitungen. *Elektrizitätswirtschaft* 65, Heft 5, 1966.
- [4] J. Pohl, Influence of high voltage overhead lines on covered pipelines. *CIGRE Paper* No. 326, June 1966.
- [5] B. Favez, J. C. Gougeuil, Contribution to studies on problems resulting from the proximity of overhead lines with underground metal pipelines., *CIGRE Paper* No. 336, June 1966.
- [6] E. D. Sunde, *Earth conduction effects in transmission systems* (Dover Publications Inc., New York, 1968).
- [7] Technical Recommendation No 7, Arbitration Agency for Problems of Interference Between Installations of the German Federal Post Office and the Association of German Power Utilities. *VHEW*, 1968.
- [8] J. Dabkowski, A. Taflove, A Mutual Design Consideration for Overhead AC Transmission Lines and Gas Pipelines. *EPRI Report EL-904*, Vol. 1, 1978.
- [9] M. J. Frasier, Power Line Induced AC Potential on Natural Gas Pipelines for Complex Rights-Of-Way Configurations. *EPRI Report EL-3106*, A.G.A. Cat. No. L51418, April 1984.
- [10] F. P. Dawalibi, R. D. Southey, Y. Malric., W. Tavcar, Power Line Fault Current Coupling to Nearby Natural Gas Pipelines, Volumes I & II., *EPRI Report EL 5472*, A.G.A., Cat. No. L51537, November 1987.
- [11] Guide on the influence of high voltage AC power systems on metallic pipelines, CIGRE Working Group 36.02, 1995.
- [12] AC corrosion on cathodically protected pipelines – Guidelines for risk assessment and mitigation measures, CEOCOR, 2001.
- [13] G. C. Christoforidis, D. P. Labridis and P. S. Dokopoulos, Inductive Interference Calculation On Imperfect Coated Pipelines Due To Nearby Faulted Parallel Transmission Lines. *Electric Power Systems Research*, Vol. 66, Issue 2, Aug. 2003, pp. 139-148.
- [14] G. C. Christoforidis, D. P. Labridis and P. S. Dokopoulos, A Hybrid method for calculating the inductive interference caused by faulted power lines to nearby buried pipelines. *To be published in the IEEE Trans. on Power Delivery*.

- [15] International Telecommunication Union, Directives concerning the protection of telecommunication lines against harmful effects from electric power and electrified railway lines, Vols. I and II, Geneva 1989.
- [16] N. Kouloumbi, G. Batis, N. Kioupis and P. Asteridis, Study of the effect of AC-interference on the cathodic protection of a gas pipeline, *Anti-Corrosion Methods and Materials*, Vol.49, No.5, 2002, pp. 335-345.
- [17] J. Weiss and Z. Csendes, A One-step finite element method for multiconductor skin-effect problems", *IEEE Trans. On Power Apparatus and Systems*, Vol. PAS-101, October 1982, pp. 3796-3803.
- [18] D. P. Labridis, Comparative presentation of criteria used for adaptive finite element mesh generation in multiconductor eddy current problems, *IEEE Trans. On Magnetics*, January 2000, Vol. 36, No. 1, pp. 267-280.
- [19] G. Papagiannis, D. Triantafyllidis, D. Labridis, A One-step finite element formulation for the modeling of single and double circuit transmission lines, *IEEE Trans. On Power Systems*, Vol. 15, Nr. 1, 2000, pp.33-38.
- [20] F. P. Dawalibi, G. B. Niles, Measurements and Computations of Fault Current Distribution on Overhead Transmission Lines, *IEEE Trans. on Power Apparatus and Systems*, Vol. 103, No. 3, March 1984, pp. 553-560.